JOM, Vol. 67, No. 12, 2015
DOI: 10.1007/s11837-015-1520-7

The Segregation Behavior of Alloying Elements in the Al-5Fe-Based Alloys During the Semisolid Deformation

LIU BO[1,2]

1.—School of Naval Architecture and Ocean Engineering, Zhejiang Ocean University, Zhoushan 316022, China. 2.—e-mail: Liubo@zjou.edu.cn

Al-5Fe-based alloys with second phases of needle-like and/or block-like morphology were prepared by thixoforming. Both microstructures and elements distribution of the alloys were investigated with scanning electron microscopy, energy dispersive x-ray spectrometry, x-ray diffraction, differential thermal analysis, differential scanning calorimetry, and compressive experiments under electromagnetic stirring and thixoformed conditions. In addition, the effect of ferro-aluminium second phases on Cu segregation in the semisolid slurry of the alloys during semisolid extrusion was investigated. The distribution and precipitation (segregation) behaviors of elements in the alloys were explored during the semisolid deformation process.

INTRODUCTION

Semisolid processing utilizes the rheological properties of metallic slurry in the mushy zone, and the semisolid pulp has better deformation capability, lower forming power, and smaller superheating and solidifying shrinkage under the action of a certain external force. It is feasible to achieve the net shape and densification of the parts. Recently, Yuan and Liu et al. have carried out research on hypereutectic Al-Fe-based alloys fabricated by the semisolid forming method, and found that semisolid processing is an effective and low-cost means for manufacturing alloys containing high volume fractions of second phases.[1,2]

During semisolid metal high-pressure die casting (SSM-HPDC), Zn, Cu, Mg, and Si elements are concentrated on the surface of SSM-HPDC plates (6 mm thick) of 7075, 2024, 6082, and A201 alloys. The contents of the above elements are above the upper limits of their specification, and reduce along the cross-section of the plates, except that the contents are slightly increased at their centers. In addition, the morphology of the intermetallic compounds in the segregated layers differs from the morphology on the surface and the center.[3] However, Cu, Zn, and Mg in the semisolid 7075 alloy are enriched in the liquid after solidification at grain boundaries and/or interglobules.[4] The grain boundaries of rheocast 7075 alloy containing only a single network eutectic phase (α-Al + η-Mg(ZnCuAl)$_2$) and a small amount of Mg_2Si phases are simpler than those of Al-Zn-Mg-Cu cast alloy.[5] In thixoformed AA6061 alloy, Cu, Mg and Si elements are more concentrated on a position of high liquid volume fraction in the part and then they are solidified in the grain boundaries and the coarse particles within grains.[6] For thixoformed A356 and A356 with 0.5 wt.% Sn alloys prepared by a strain-induced melt-activated (SIMA) method, using a subliquidus casting and magneto-hydrodynamic technique, the globular structure is less segregated than the dendritic structure. The rounder grains and the smaller granular size, and the lower segregating degree occur during thixoforming.[7] The intra-granules of thixocast 356 alloy containing 0.5 wt.% Fe produced by electromagnetic stirring are composed of Al and a small quantity of Mg, and lamellar Si and Mg_2Si particles constituting the eutectic regions are located between the globules containing the Fe-rich and Mg-rich compounds.[8] In the thixoformed 201 alloy, Cu, Mg and Si elements are only gathered together between the globules. The scale of the microstructure is similar to that concentrated between the dendrites of the permanent mold-cast 201 alloy. However, the liquid enriching the alloying elements in thixoformed 2014 alloy aggregates between the globules and within the grains during thixoforming.[9] Thus, it can change the grain boundary chemistry and facilitate the forming of a ternary Al-Cu-Si eutectic with a lower melting-point at the grain boundaries.[10] This leads to a lack of Cu inside the grains and the solidus of the alloy is reduced.[11]

(Published online July 1, 2015)

Moreover, only 1 at.% Cu is contained in the α-Al granules and most of the alloying elements are congregated in the eutectic regions between the globules, or within the globules for the thixocast 319 alloy.[12]

Reference 13 has numerically simulated the extrusion of semisolid materials with the solid fraction of 0.63 in a container. At the initial deformation stage (up to 35% of height reduction), the extrusion pressure is mainly supported by the solid, and the liquid pressure inside the interstices (pore pressure) is two orders of magnitude lower than the extrusion pressure. With the increase in the deformation (35–45% of height reduction), both the pore pressure and the extrusion pressure increase rapidly. The increasing ratio of the pore pressure is several times higher than that of the extrusion pressure. When the height reduction is above 45%, the extrusion pressure becomes constant, which means that a steady state has been achieved, but the pore pressure goes on increasing. Notably, the liquid within the closed areas in the mushy zones will solidify under the higher pressure during semisolid squeezing. In addition, the liquid is inclined to flow toward the die exit before the steady state, and flows toward the position under relatively low pressure in the regime after the steady state. These results are similar to our previous experimental investigations.[14,15]

Unlike the microstructure of conventional semisolid Al alloys, the typical microstructure of semisolid Al-5Fe-based alloys is composed of the nearly spherical parent solid solution (α-Al granules), and lamellar and blocky heterogeneous solid (AlFe second phases), which are suspended in the liquid, i.e., consisting of two miscellaneous solids and a liquid in the liquid–solid regime. Thus, the semisolid deformational behavior of the alloys is different from that of conventional semisolid Al alloys. The segregation of the elements in conventional semisolid Al alloys has been extensively studied,[4,5,8,9,12] in which it is considered that the low-melting compounds or eutectic phases re-melted in the solid–liquid zone induces the redistribution of solutes during solidification, resulting ultimately in the segregation of their constituted elements. Nevertheless, the elements segregating for the alloys consist of two miscellaneous solids and a liquid, which has the characteristics of it compared with conventional semisolid Al alloys when semisolid-forming, is also seldom reported. In this paper, we focus on the origin of alloying elements segregating in Al-5Fe-based alloys during semisolid deformation. Because the microstructure of the alloy depends powerfully on the semisolid processing procedure, in order to explore the impacts of the heterogeneous second phases on the elements segregating and the phase formation, the thermal simulation experiment of semisolid compression is also examined alongside thixoforming.

EXPERIMENTAL

The compositions of Al-5Fe-based alloys used in this paper are provided in Table I. A common smelting process is adopted and has been described in detail in Ref.1 Because Alloy 11 is slightly different in constituents from Alloy 156, we can study the effect of diverse contents and shapes of AlFe second phases on alloying segregation. The alloy billets prepared by electromagnetic stirring were machined into two cylindrical specimens (63 mm in diameter and 70 mm in height, and 8 mm in diameter and 12 mm in height, respectively). The former was used for thixoforming parts and the latter was used for thermal simulation experiments of semisolid compression.

To prevent the extruded molten metal falling from the specimen in the compressing experiment, vertical compression was employed. An INSTRON universal testing machine (Instron-5500R; Illinois Tool Works, USA) was used in the experiment. The testing temperature range was from 610°C to 650°C. Through differential thermal analysis (DTA) with a Dupont-1090 apparatus (Du Pont de Nemours, USA), the liquidus and the solidus of Alloy 11 and Alloy 156 were measured to be 649.9°C and 505.2°C, and 656.7°C and 515.4°C, respectively. Differential Scanning Calorimetry (DSC) measurements were also performed by using a TA Q100 DSC Differential Scanning Calorimeter system (TA Instruments, USA) with a heating rate of 10°C/min. Compressional decrements were, respectively, 2.4 mm, 6 mm, and 10 mm, and the corresponding true strains (ε) were 0.22, 0.69, and 1.79, respectively. The strain rates ($\dot{\varepsilon}$) were 5×10^{-3} s, 1×10^{-2} s, 1×10^{-1} s, and 5×10^{-1} s, respectively.

A vacant resistant furnace equipped on the Instron-5500R tester was first heated to a scheduled testing temperature, and then the specimen was placed in the furnace, reheated to the required temperature and maintained for 5 min before the compressing test was carried out. In the vacant resistant furnace, the temperature control was realized with three thermocouples and the control accuracy was ±1°C. The experimental data were automatically collected by a computer on the tester.

Table I. Composition of experimental Al-5Fe-based alloys (wt.%)

Alloy	Fe	Cu	Zn	Cr	Mn	Mg	Zr	Ti	B	Si	Al
11	6.82	3.74	2.69		0.49	0.21		0.12	0.01	<0.2	Bal.
156	5.87	4.23	0.51	2.03	0.53	0.34	0.32	0.11	0.0096	<0.2	Bal.

In order to reduce the friction force between the specimen and the indenter of the tester, a few graphite powders were coated on the head face of specimen, so that the influence of the friction force on the true stress could be minimized in the experiment. After compression, the specimen was quickly quenched by cooling water.

For the thixoforming parts, cylinders with the size of ϕ 63 mm $\times$ 70 mm from the electromagnetic stirred billets were heated at 630°C for 30 min in a box-type electric furnace (KOYO-52878; Koyo Thermo Systems, Japan) before extruding into a cake with the diameter of 84 mm and the height of 24 mm using a hydraulic machine (YH615-500;HFM,Hefei,China). The imposed extrusion forces were 1800 kN–2500 kN. The pressurized time was about 5 min and the extruded speed was 2 mm s^{-1}. The extrusion ratio was 8:1 and corresponding true strain was 4.16.[16]

The compressed specimen was cut along the forced direction (in a direction perpendicular to the compressional face) and the thixoformed sample from the cakes before the metallographic sample was ground and polished or etched by Keller solution or 5% HF. The microstructure was observed with an optical microscope (OM) (BX60 M; Olympus, Japan) and a scanning electron microscope (SEM) (S-3400N; Hitachi, Japan), which was equipped with an energy dispersive x-ray spectrometer (EDS) to analyze the chemical constitution of the phases in the alloys. Moreover, the phases were identified by an x-ray diffractometer (XRD) (D8 Discover; Bruker, Germany) using a Cu $K_{\alpha 1}$ target.

RESULTS AND DISCUSSION

The microstructure of the Al-5Fe-based alloys prepared by electromagnetic stirring is shown in Fig. 1. The structure is composed of blocky and sheet-like Fe-rich second phases with a length less than 250 μm, reticular Cu-rich compounds, and near globular as well as much dendritic α-Al. The iron-rich phases composed of needle-like or sheet-like brittle phases in Alloy 11 and blocky and flaky phases in Alloy 156 become shorter and finer and distribute more evenly compared with the as-cast microstructure.[1] The dendritic structure was smothered or eliminated so that the grains tended to be distinctly round, and there was a significant refining effect of electromagnetic stirring on the alloys' microstructure. Furthermore, the content of AlFe phases in Alloy 156 was higher than that in

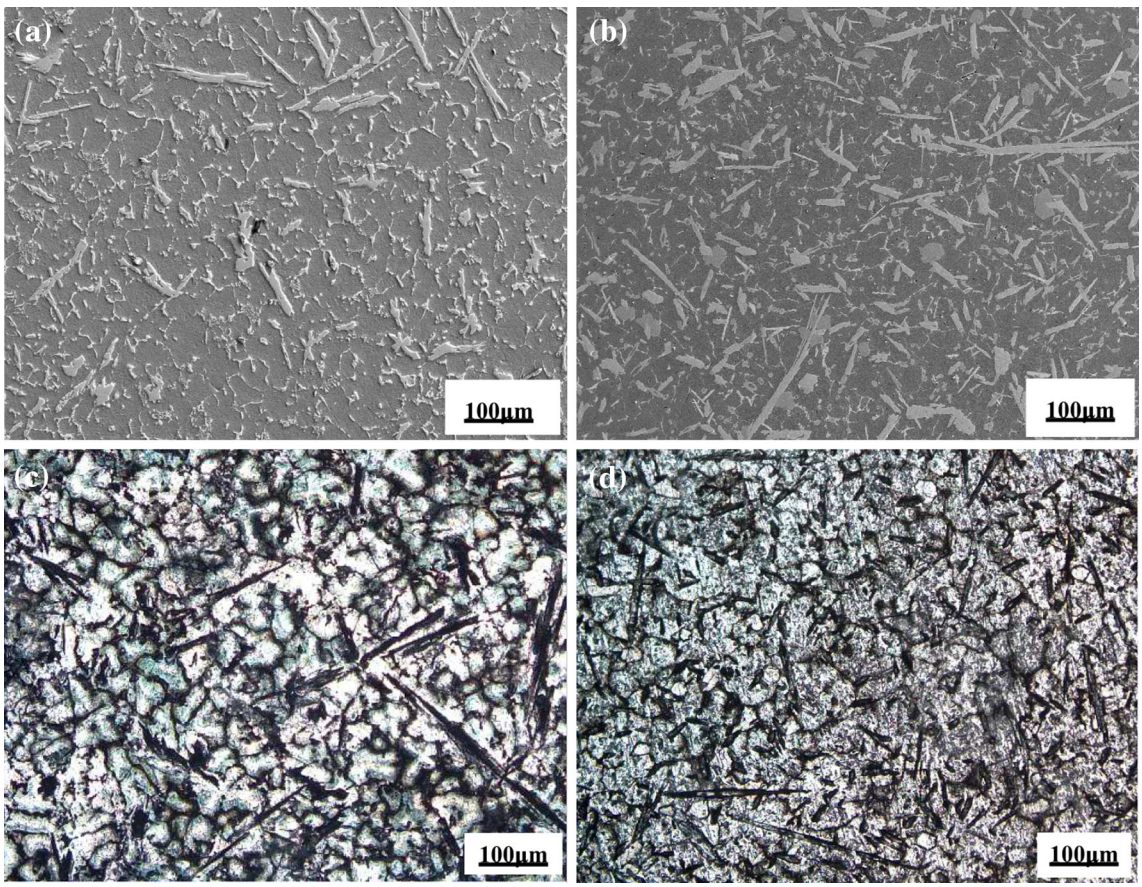

Fig. 1. Electromagnetic stirred microstructure of Al-5Fe based alloys, (a), (c) Alloy 11; (b), (d) Alloy 156; (a), (b) SEM image; (c), (d) OM image, Keller's etched.

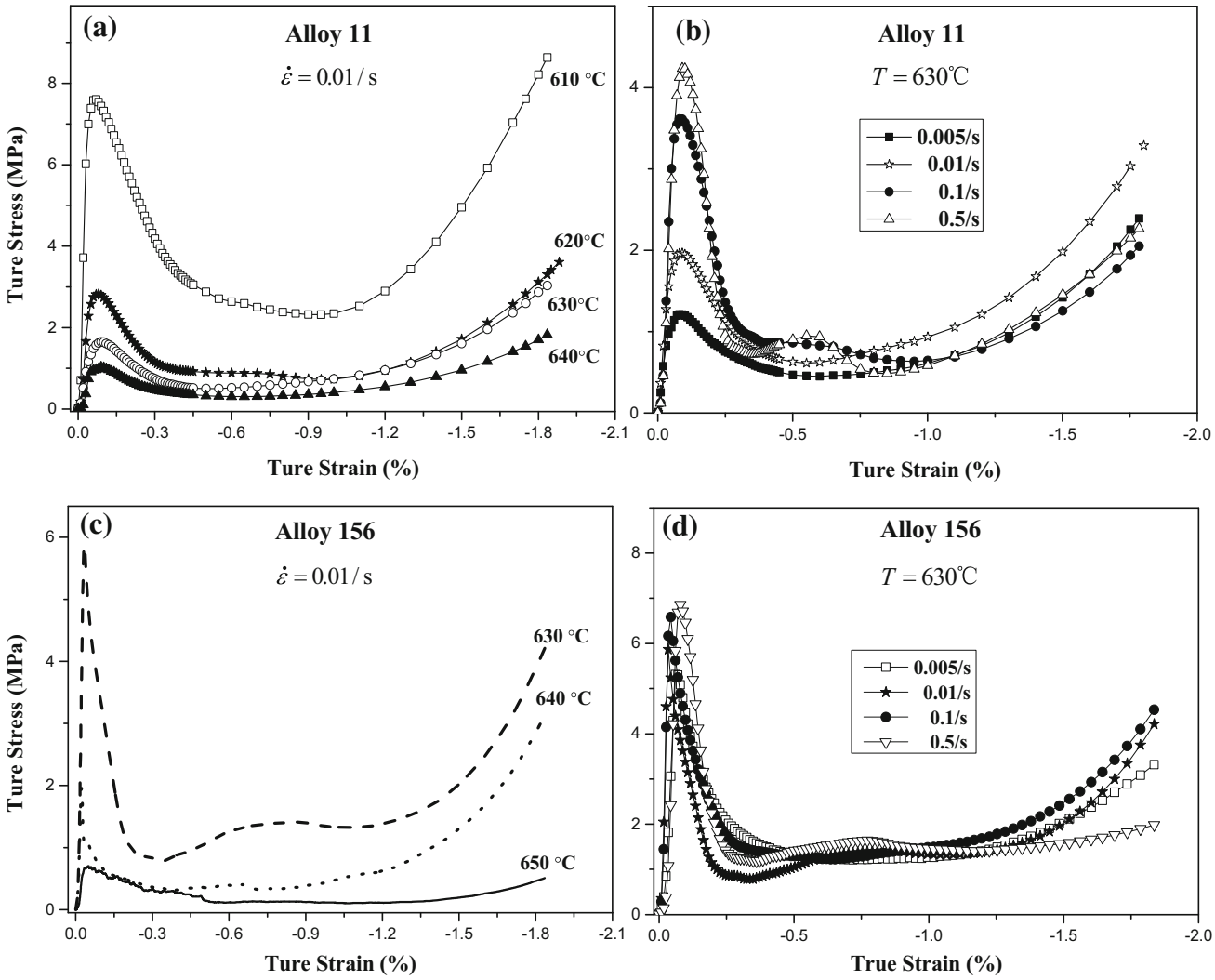

Fig. 2. True stress–strain of Al-5Fe-based alloys deformed at various temperatures and strain rates (ε = 1.79).

Alloy 11 because Alloy 156 contained more elements of generating intermetallics such as Cr, Zr. The morphology of AlFe phase containing Cr grew mostly blocky and ring-like because Cr dissolved only in the $Al_{13}Fe_4$ phase.[17] The number of reticulations in Alloy 156 dropped significantly at the same time.

Figure 2 illustrates the true stress–true strain curves of the semisolid formed Al-5Fe-based alloys compressed by the strain rate ($\dot{\varepsilon}$ = 0.01 s) for different temperatures (Fig. 2a and c) and by various strain rates at 630°C (Fig. 2b and d). The flow stress of the semisolid deformed Al-5Fe-based alloys increased significantly with decreasing the deformation temperature (Fig. 2). However, the true stress–true strain curve of the alloys is typically characterized by a peak flow stress and followed by a stable flow stress. Strain softening occurred during the semisolid compression of the alloys.[14]

During the semisolid deformation of the alloys, the second phases, such as AlFe compounds and other intermetallic compounds, must move and rotate to accommodate the deformation of the matrix. When the alloys compressed with a strain rate of 0.01 s^{-1} in the mushy zone, the molten phase appeared preferentially at the grain boundaries or around these compounds, where it could serve as a lubricant for the redistribution of the compounds and the grains. In the low-temperature deformation, which corresponded to the small volume fractions of liquid, the liquid wetted the grain boundaries with a thin film that was solidified epitaxially and the liquid segregation resulted in a significant increase in the peak flow stress. Meanwhile, the matrix offered less resistance to the second phase redistribution. With elevating the deformation temperature, the liquid adequately wetted the grain boundaries or the second phase/matrix interface and contributed to the load transferring from the matrix to the compounds, resulting in the decline of the flow stress (Fig. 2a and c). In addition, when the alloys deformed at 630°C, the longer distribution time allowed the liquid to be

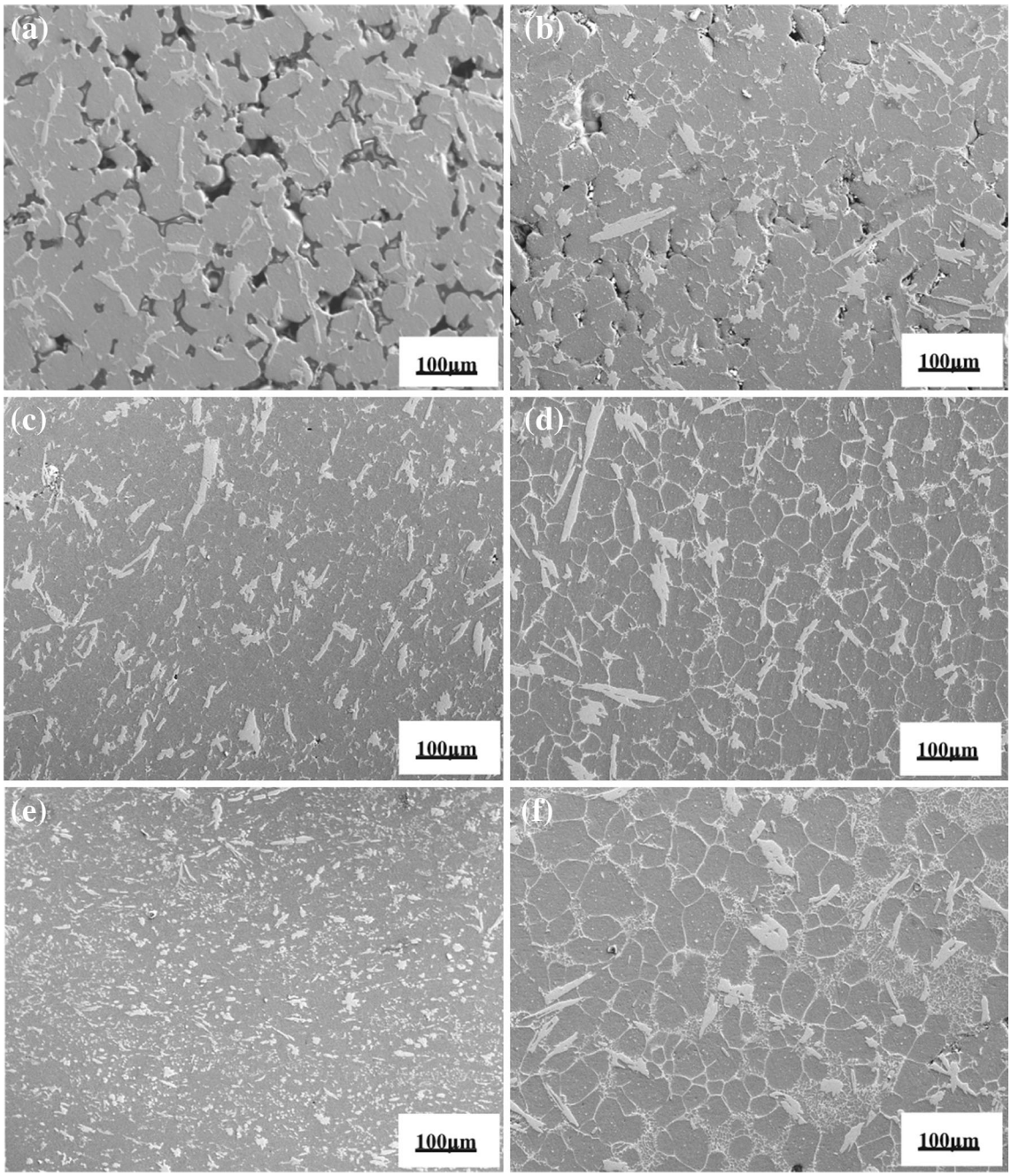

Fig. 3. Microstructure of the center in Alloy 11 specimens at different temperatures and strains ($\dot{\varepsilon} = 0.01\,s^{-1}$). (a), (c), (e) 610 °C, (b), (d), (f) 640 °C and (a), (b) ε = 0.22, (c), (d) ε = 0.69, (e), (f) ε = 1.79 (adapted from Ref.14).

distributed to the grain boundaries or around the compounds with decreasing the strain rate, thus leading to the lubrication of the liquid and the decrease in the flow stress (Fig. 2b and d). Therefore, the redistribution and breakage of the intermetallic compounds are responsible for the significant strain softening of the Al-5Fe-based alloys.

Figure 3 shows the microstructure in the center of Alloy 11 specimens under various temperatures and strains ε. The irregular grains entered the nearby globules. With increasing the deformation temperature, the inconspicuous and intermittent grain boundaries were transformed into distinct and continual reticulations or Chinese scripts, and the width of the grain boundaries was also increased. The grayish reticulations were AlCuFe compounds consisting of Al_7Cu_2Fe phase and/or Al_2Cu phase, with or without Fe according to EDS, indicating that Cu and Fe tended to be concentrated on the grain boundaries to form cupriferous

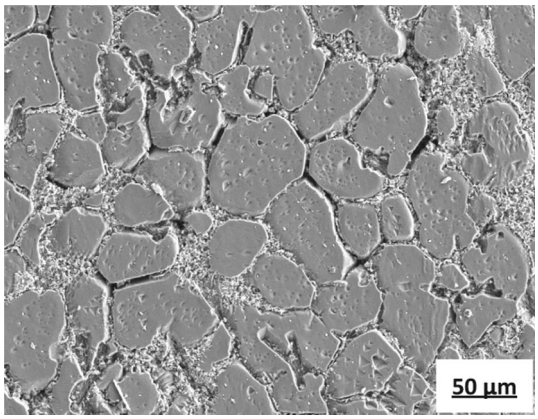

Fig. 4. Microstructure of Alloy 11 compressed at 640 °C, strain rate $\dot{\varepsilon} = 0.1\,s^{-1}$ and true strain $\varepsilon = 0.69$. It is obvious that wider ditches and thin reticular Cu-rich regions have remained between grains because Cu-rich compounds on grain boundaries or inter-grains were etched by 5% HF aqueous solution.

compounds when the deformation temperature increased. Cu content on the grain boundaries was higher than that within the grains (1.37–2.04 at.%). Moreover, the cupriferous compounds on the grain boundaries grew from the sparse and inchoate network under the small deformation to the dense and reticular morphology at the large deformation with increasing the deformation. When the deformation increased further, the retiform cupriferous compounds were transformed into the dense and fine reticulary Chinese-script structure (Fig. 3b, d, and f). This indicated that the decrease in the flowing channels of the liquid and the increase in the flowing resistance during increasing the deformation compels the liquid to remain in the flowing impeded position leading to the liquid segregation. Furthermore, the microstructural evolution of Alloy 156 is similar to that of Alloy 11 during semisolid deformation.

The liquid fraction increased with increasing the deformation temperature. When solid particles were surrounded by the liquid, with the liquid acting as a lubricant, the solid particles could slide, turn, or move along the liquid membrane to adjust the deformation resulting in decreasing the flow stress.[14] Because there were high volume fractions of lamellates or blocky high-melting AlFe second phases in the Al-5Fe-based alloys, these solids would be difficult to be entirely encircled by the liquid and could resist the liquid flowing during compression. The liquid would remain there due to flowing suffocation and this would enhance the segregation of the liquid. However, the liquid in the areas with the small quantity of AlFe second phases would flow among the grains along the flowing channels. Once the channel had formed, the channel could widen gradually and the liquid lubrication would be enhanced, resulting in decreasing the flow stress in the process of compression.[18] Finally, it was solidified into reticular cupriferous sediments to broaden the grain boundaries (Fig. 4), and the liquid was trapped within the grains during semisolid remelting to solidify the granular Cu-rich compound with or without Fe. Furthermore, when the compressive deformation increased further, the solids contacted each other and plastic deformation occurred. The flowing channels were blocked and the liquid gathered where liquid flowing had been prevented, forming cupriferous compounds with the shape of Chinese characters made up of fine grids.

As shown in Fig. 5, the grains in Alloy 11 gradually become round and loose. The grayish cupriferous precipitation is becoming a network with increasing the strain rate during compressional deformation at 640°C for the strain of 0.69. When the strain rate increased above $0.01\,s^{-1}$, most reticular cupriferous precipitations are widened and transformed into the Chinese-script structure with small grids, and the roundness of the grains reduces again. The grains are transformed into irregular and non-uniform shapes and the grain boundaries also beocme discontinuous and indistinct. The reticular cupriferous precipitations are crushed or scattered. The number of the precipitations decreases significantly when the strain rate is further increased (Fig. 5c and d).

The precipitation of Cu, Fe and other elements in Al-5Fe-based alloys during semisolid deforming is illustrated in Fig. 6. With increasing the deforming temperature, the Al_7Cu_2Fe compound on the grain boundaries and/or around the AlFe phase is converted from the intermittent network to the continuous network, and the Chinese-script structure with fine grids is formed in the liquid accumulation areas. As the strain increases, the grains are contacted and squeezed with each other and plastic deformation of the solid occurs. The (Cu, Fe)-rich liquid parceled within the grains is finally solidified to form the granular Al_2Cu phase containing Fe or Mn (Fig. 6a and c). The result is similar to previous results.[9] Comparing Fig. 6a with Fig. 6c, it can be seen that the grains in Alloy 156 containing more second phases are finer than those in Alloy 11, although the deformation degree of Alloy 156 is smaller, indicating that the second phases can restrain the grain coarsening during semisolid machining. Of course, more intermetallic compounds in Alloy 156 would require a higher flow stress for deformation. Furthermore, it can be observed in Fig. 6 that some phases have been cracked and even broken at the high temperature. The blocky AlFe phase with high Cr (~6.84 at.%) in Alloy 156 and the lamellate AlFe phase without Cr in Alloy 11 are denser than the sheet AlFe phase containing low Cr (~2.87 at.%) in Alloy 156. This reveals that the structure of the sheet AlFe phase with low Cr is different than that of the blocky AlFe phase with high Cr. The thermal strength of the former is less than that of the latter or lamellate-free Cr AlFe phase.

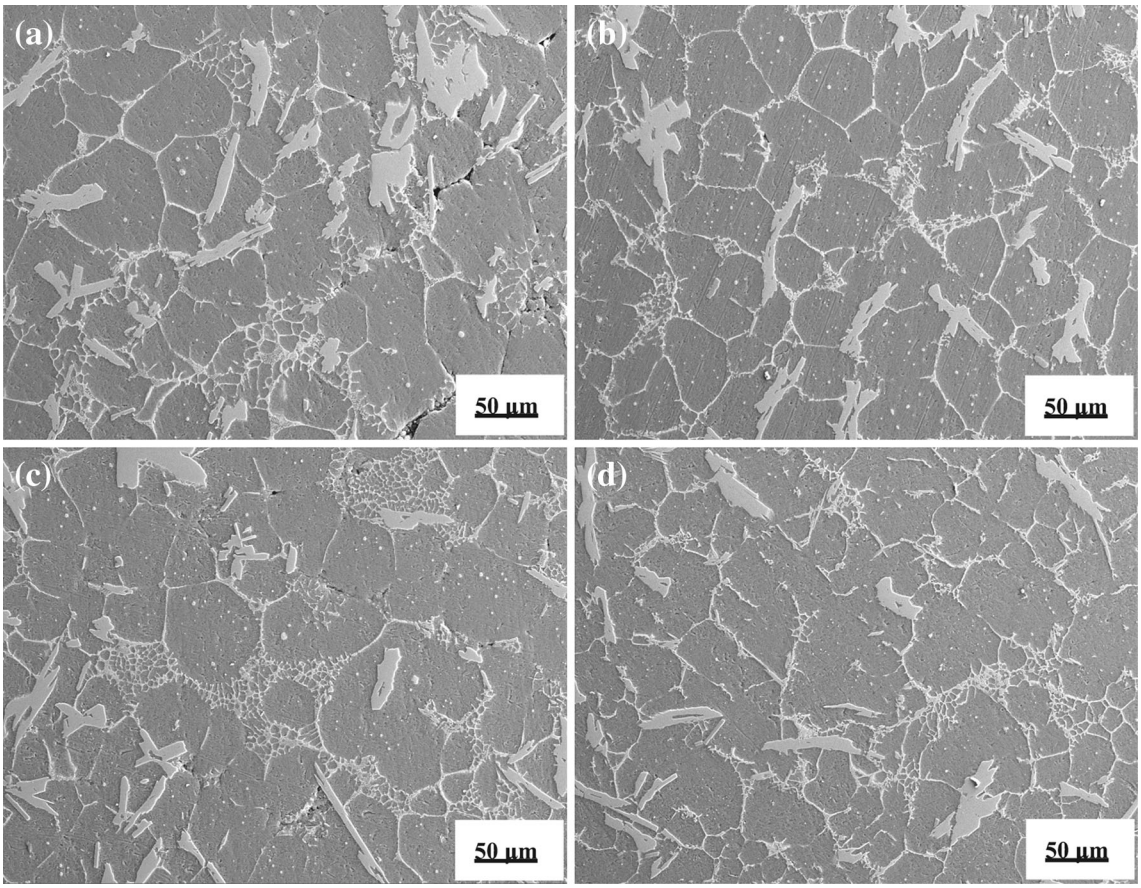

Fig. 5. Microstructure of Alloy 11 deformed at different strain rate (T = 640 °C, ε = 0.69). (a) $\dot{\varepsilon} = 0.005\,s^{-1}$, (b) $\dot{\varepsilon} = 0.01\,s^{-1}$, (c) $\dot{\varepsilon} = 0.1\,s^{-1}$, (d) $\dot{\varepsilon} = 0.5\,s^{-1}$.

As shown in Figs. 3 and 6, the higher the liquid fraction in the semisolid alloys, the more the AlCuFe precipitation. The precipitated distribution is almost consistent with the liquid distribution during semisolid deforming, indicating that the precipitation of Cu and Fe elements is closely related to the distribution of the liquid in Al-5Fe-based alloys during semisolid deformation. Distinctly, during semisolid re-melting, Cu in Al-5Fe-based alloys can diffuse to the liquid at high temperature besides re-dissolving into the matrix, and the dissolution of the low-melting Al_2Cu and Al_7Cu_2Fe compounds will also make the liquid become more enriched with elements such as Cu and Fe, resulting in the contents of Cu and Fe in the liquid outweighing those in the solid. Cu, Fe and other elements accumulated in the liquid will form binary or multivariate cupriferous compounds containing other elements, or be transformed into the Cu-rich region in subsequent solidification. Consequently, the liquid flow can directly reflect the precipitation of the elements such as Cu and Fe under the various semisolid deformations. In other words, research on the distribution of Cu, Fe, and other elements in
Al-5Fe-based alloys may reveal the flow track of the liquid in semisolid deforming, ascertain the influence of the liquid on the semisolid deformation and then understand the elements segregation.

During the semisolid deformation, the liquid can flow along the flowing channel under extrusion and finally accumulate in inter-granules or around AlFe phases which the flowing had hindered. The (Cu, Fe)-rich liquid assembled around the AlFe phases will form a structure where the Al_7Cu_2Fe compound is attached around or in the interstice of the $Al_{13}Fe_4$ phase as a nucleating core. In Fig. 7, a few independent light gray Al_7Cu_2Fe compounds are distributed in the α-Al matrix of as-thixoformed Alloy 11. The light gray compound attached to the side of the dark grey $Al_{13}Fe_4$ phase is crosswise connected by the flakiness at Point A. In the microstructure of Al-5Fe-based alloys, the Al_7Cu_2Fe compound is mainly attached to the edge of the $Al_{13}Fe_4$ phase (Point B), where the acicular compound sticks to the interior of the $Al_{13}Fe_4$ phase and around the dendrite of the phase rather than in the α-Al matrix. The structure differs from that at Point A. Such a microstructure is the result of a peritectic reaction: $L + Al_{13}Fe_4/(AlCu)_{13}(FeMn)_4 \leftrightarrow Al_7Cu_2Fe/Al_7Cu_2(FeMn)$. The reaction can lead to the disappearance of the $Al_{13}Fe_4$ in the case of equilibrium solidification. However, when the solidification is dominated by the Scheil model (i.e. the diffusion does not occur

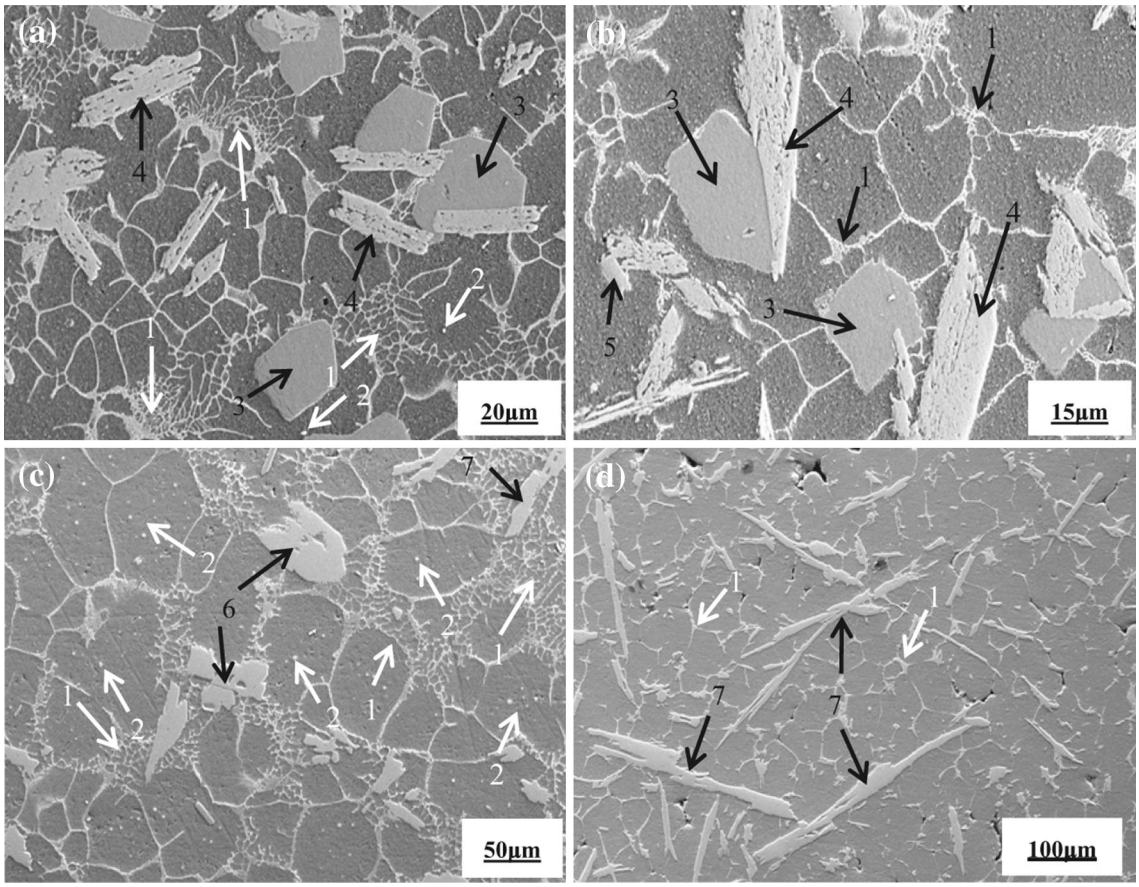

Fig. 6. The distribution of phases in Al-5Fe-based alloys under various deformation ($\dot{\varepsilon} = 0.01\,s^{-1}$). (a) Alloy156, T = 650 °C, ε = 0.22, (b) Alloy156, T = 640 °C, ε = 0.22, (c) Alloy11, T = 640 °C, ε = 1.79, (d) Alloy11, T = 610 °C, ε = 0.22.

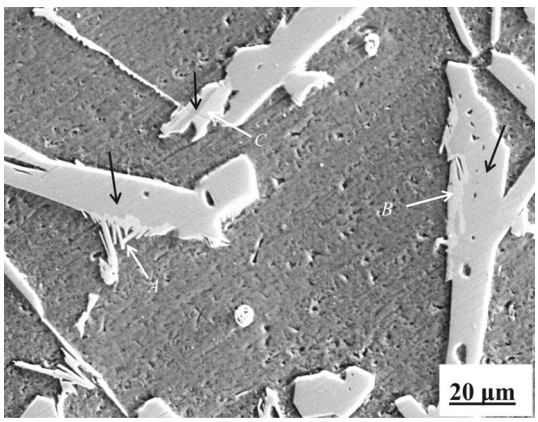

Fig. 7. Evolution of Al_7Cu_2Fe compound around $Al_{13}Fe_4$ phase in Alloy 11 semisolid formed, white arrows signify Al_7Cu_2Fe and the black arrow is $Al_{13}Fe_4$ phases with Cu and Mn.

in the solid state), the transformation from the $Al_{13}Fe_4$ phase precipitating to the Al_7Cu_2Fe compound forming occurs only at the peritectic point. In this case, the phase formed at the lower temperatures will surround the phase formed at the higher temperatures. The large area of light gray Al_7Cu_2Fe compound wraps around the dark grey $Al_{13}Fe_4$ to form a "core–shell" structure (Point C). It can be concluded that (Cu, Fe)-rich liquid around the $Al_{13}Fe_4$ phase can transform the Al_7Cu_2Fe compound through a peritectic reaction under a certain condition during thixoformation. This implies that the Al_7Cu_2Fe compound can nucleate on the faceted $Al_{13}Fe_4$ phase which has edges and corners in the concave and is easier to adsorb atoms and serve as a nucleating substrate. An AlFeSi intermetallic nucleated on the $Al_{13}Fe_4$ phase was discovered in the Al-Mg-Si wrought alloy.[19] The Al_7Cu_2Fe compound attached around the AlFe phases is mainly generated by the above peritectic reaction, whereas a small amount of Al_7Cu_2Fe compound distributed independently in the α-Al matrix is produced by another peritectic reaction: L + Al_6(FeCuMn) ↔ Al + Al_7Cu_2Fe. In addition, the liquid containing Cu and Fe among the grains will form binary or multivariate Cu-bearing compounds or be solidified into the Cu-rich region. The EDS analysis shows that the cupriferous compounds consist of Al_7Cu_2Fe and Al_2Cu compounds with or without Fe. In the as-thixoformed Al-5Fe-based alloys, the primary α-Al presents a near-globular morphology and the AlFe second phase displays an acicular and blocky structure. A cupriferous compound and/or the

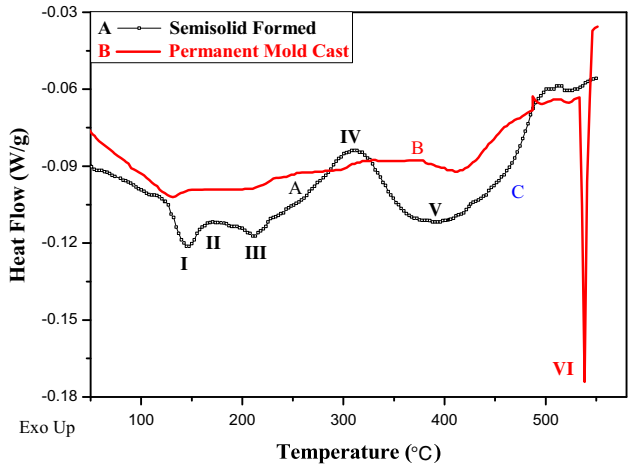

Fig. 8. DSC thermogram of Alloy 11 under different processing conditions: A semisolid formed, B permanent mold cast.

Cu-rich region (Cu segregated region) solidified from the liquid in the semisolid slurry is located in interglobular regions, around the AlFe phases and within the globules.

During DSC heating and cooling, the precipitation and dissolution reactions in the sample can be reflected by a number of heat effects shown in the DSC curves. Figure 8 shows the typical DSC curves of the Al-5Fe-based alloys prepared under different processing conditions. According to previous results of conventional Al-Cu alloys after solutionizing,[20–24] the heat effects are identified as follows: Peak I corresponds to the dissolution of GP I or solute cluster, Peak II corresponds to the formation of GP II or θ'' phase, Peak III corresponds to the dissolution of θ'' phase. Effects IV and V are ascribed to the formation and dissolution of θ' phase, respectively. Effect VI corresponds to the melting of θ-Al_2Cu stable phase or AlCuFe compounds and is distinctly observed in a DSC curve of the as-permanent-cast Al-5Fe-based alloy (Curve B) but nearly disappears in the DSC curve of the as-semisolid-formed alloy (Curve A). The narrow and sharp Peak VI in Curve B is much greater than that in Curve A, indicating that the Cu element is mainly in the form of a compound such as θ-Al_2Cu in the as-cast Al-5Fe-based alloy unlike the as-thixoformed alloy. From the temperature record curves, meaningful information arises, such as the area under the curve, peak temperature, and full-width at half peak height in an endothermic or exothermic peak, which are, respectively, related to the volume fraction of the precipitation, average precipitate size, and precipitate size distribution. These DSC results imply that the microstructure of semisolid formed Al-5Fe-based alloys is equivalent to that of conventional Al-Cu alloys after solutionizing. Cu in the alloy can redissolve in the α-Al matrix to produce the supersaturated solid solution during semisolid machining. This is consistent with the XRD results that the content of Al_2Cu compound in Al-5Fe-based alloys is reduced from 19.6% in the as-permanent-cast alloy to 0.4% in the as-semisolid-formed alloy. Distinctly, when semisolid compressional deformation occurs to a certain degree, the liquid within the closed regions (within pores) in the slurry will bear the pressure which is several times higher than the extrusion pressure, and the solid around the regions can also sustain the same reactive force,[13] so that these solids undergo the larger deformation. Consequently, the semisolid extrusion displays a stress amplification effect for the isolated and sealed liquid regions in semisolid slurry of the alloy. Because the solid framework composed of AlFe phases in the alloys is stronger in the mushy zone and can bear a higher reactive force so as to extend the existing period of the closed regions, the stress effects will be further amplified to make the liquid solidify under the higher pressure. When the liquid crystallizes under pressure, there is not enough time for the solute element in the alloys to precipitate and easily form a supersaturated solid solution due to the increase in the solidifying rate of casting and the slowing of the diffusing rate of the solute. Therefore, the alloys' solidified structure contains more Cu solute and is similar to the as-quenched microstructure of conventional Al-Cu alloys.

Visibly, the liquid segregation is a characteristic of semisolid forming no matter whether it is applied in conventional casting alloys or in wrought alloys.[3] The segregation behavior of all alloys is closely related to their microstructures. The degree of segregation depends on the alloy composition, die structure, and processing parameters.[3,7] The liquid segregation can result in the elements accumulating where the liquid flow had hindered during semisolid forming, thus leading to the non-uniform microstructure and the varying mechanical properties of the formed parts.

CONCLUSION

In the process of semisolid deforming, Cu is enriched in the liquid of the slurry of Al-5Fe-based alloys. The dissolution of low-melting Al_2Cu and/or Al_7Cu_2Fe compounds also makes the liquid segregate more Cu, Fe, and other elements.

High-melting AlFe second phases impede the liquid flow resulting in the liquid segregation. The deterred liquid remained around the second phases, among the globules, or in the intra-granules during extrusion. The liquid around the AlFe phases will solidify into a structure in which the Al_7Cu_2Fe phase is attached around or to the gaps of the $Al_{13}Fe_4$ phase and serves as a nucleating core forming a Chinese script-like AlCuFe compound or Al_2Cu phase with or without Fe among the grains. Furthermore, a small amount of the liquid in the intra-globules is transformed into a granular Al_2Cu compound with or without Fe.

During semisolid deforming, the cupriferous compounds are first gathered gradually on the grain boundary and transformed from the discontinuous to a continuous network or Chinese-script shape,

and then the net-like or Chinese script-like compounds on the grain boundary are crushed and the grain boundary becomes discontinuous and indistinct again with increasing the deformation temperature, strain rate and deformation. Precipitation of the more retiform cupriferous compounds broadens the grain boundary. The Cu-rich compounds are mainly $Al_7Cu_2Fe/Al_7Cu_2(FeMn)$ compound and/or slight Al_2Cu phase containing Fe.

The liquid can solidify under the higher pressure due to the existing solid AlFe framework in the semisolid slurry, resulting in more solute Cu dissolving in the matrix to form a supersaturated solid solution during semisolid forming.

The distribution of Cu and Fe elements in semisolid formed Al-5Fe-based alloys is directly related to the liquid flow path during semisolid forming. From research on Cu and Fe elements distributed in the alloys during semisolid processing, we can ascertain the track of the liquid flowing in semisolid deformation and understand the effect of liquid fraction on semisolid deformation.

ACKNOWLEDGEMENTS

The paper is supported by Zhejiang Ocean University Research start-up funds (Grant No. 21045012513).

REFERENCES

1. B. Liu, X.G. Yuan, and H.J. Huang, *China Foundry*, 8(4), 259 (2011). http://www.foundryworld.com/english/foundry/old.asp?types=6&leib=2&Years=2011&months=4.
2. X.G. Yuan, S.G. Zhao, S. Li, Y.J. Lu, and H.J. Huang, *Foundry* 55, 466 (2006).
3. H. Möller, U.A. Curle, and E.P. Masuku, *Trans. Nonferrous Met. Soc. China* 20, 847 (2010).
4. H.V. Atkinson, K. Burke, and G. Vaneetveld, *Mater. Sci. Eng. A* 490, 266 (2008).
5. N. Mahathaninwong, T. Plookphol, J. Wannasin, and S. Wisutmethangoon, *Mater. Sci. Eng. A* 532, 91 (2012).
6. S.Y. Lee and S.I. Oh, *J. Mater. Process. Technol.* 130–131, 587 (2002).
7. E.A. Vieira and M. Ferrante, *Acta Mater.* 53, 5379 (2005).
8. P. Cavaliere, E. Cerri, and P. Leo, *J. Mater. Sci.* 39, 1653 (2004).
9. D. Liu, H.V. Atkinson, P. Kapranos, and H. Jones, *J. Mater. Sci.* 39, 99 (2004).
10. Y. Birol, *Mater. Sci. Eng. A* 528, 5636 (2011).
11. Y. Birol, *J. Mater. Process. Technol.* 211, 1749 (2011).
12. E. Cerri, E. Evangelista, S. Spigarelli, P. Cavaliere, and F. DeRiccardis, *Mater. Sci. Eng. A* 284, 254 (2000).
13. S. Toyoshima and Y. Takahashi, *ISIJ Int.* 31, 577 (1991).
14. B. Liu, X.G. Yuan, H.J. Huang, and S.H. Zhang, *Adv. Mater. Res.* 152–153, 726 (2011).
15. B. Liu, X.G. Yuan, S.H. Zhang, and H.J. Huang, *J. Plast. Eng.* 16, 11 (2009).
16. J. Zrnik, S.V. Dobatkin, and I. Mamuzič, *METABK* 47, 211 (2008).
17. B. Liu, X.G. Yuan, H.J. Huang, and Z.Q. Guo, *JOM* 64, 316–322 (2012).
18. S.J. Luo, Y.S. Cheng, and W.W. Shan, *Rheology of Semisolid Metal* (Beijing: National defense industry press, 2011), p. 116.
19. M. Hosseinifar and D.V. Malakhov, *Metall. Mater. Trans. A* 42A, 825 (2011).
20. M. Takeda, S.K. Son, Y. Nagura, U. Schmidt, and T. Endo, *Z. Metallkd.* 96, 870 (2005).
21. S.K. Son, M. Takeda, M. Mitome, Y. Bando, and T. Endo, *Mater. Lett.* 59, 6292 (2005).
22. D. Larouche, C. Laroche, and M. Bouchard, *Acta Mater.* 51, 2161 (2003).
23. C. García Cordovilla and E. Louis, *J. Mater. Sci* 19, 279 (1984).
24. Y.H. Shang Guan, J.F. Wang, D.S. Zhang, and Z.X. Liu, *Foundry Technol.* 31, 888 (2010).